Macromolecules



Article

# Gel Processing for Highly Oriented Conjugated Polymer Films

Daniel Alcazar, Fei Wang, Timothy M. Swager, and Edwin L. Thomas

*Macromolecules*, **2008**, 41 (24), 9863-9868 • DOI: 10.1021/ma8020739 • Publication Date (Web): 21 November 2008



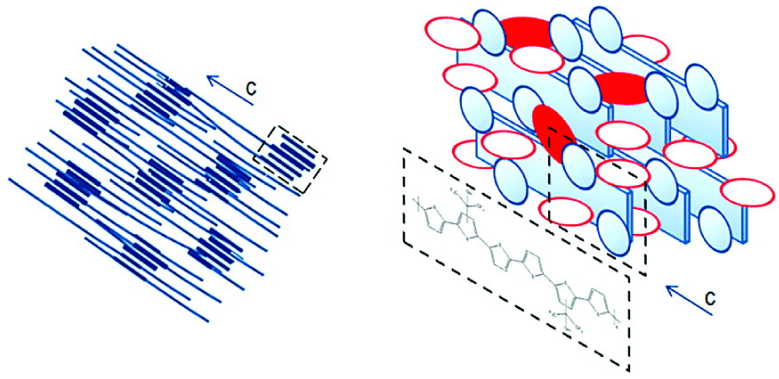


## More About This Article

Additional resources and features associated with this article are available within the HTML version:

- Supporting Information
- Access to high resolution figures
- Links to articles and content related to this article
- Copyright permission to reproduce figures and/or text from this article

View the Full Text HTML

# Gel Processing for Highly Oriented Conjugated Polymer Films

**Daniel Alcazar,[†] Fei Wang,[†] Timothy M. Swager,[‡] and Edwin L. Thomas*,[†]**

*Department of Materials Science and Engineering and Department of Chemistry, Massachusetts Institute of Technology, Cambridge, Massachusetts 02139*

*Received September 11, 2008; Revised Manuscript Received October 29, 2008*

ABSTRACT: Hexafluoroisopropanol functionalized polythiophene is able to build up an isotropic self-supporting network structure. The gel network can be melted and then transformed via mechanical shearing to form an anisotropic gel with the chains highly aligned along the shearing direction and the conjugated backbones $\pi$-stacked with respect to each other neighbors. The mechanism by which a dipole functionalized polythiophene can form a reversible network able to be deformed into structurally oriented films may be of interest in the development of novel processing routes for conjugated polymers.

## Introduction

In recent years, there has been an increased interest in using conjugated polymer materials for commercial applications. Intrinsic electrical conductivity and electroluminescence along with the potential for further functionalization allow conjugated polymers to be competitive candidates for transistors, light-emitting diodes and sensors.[1] Polythiophenes are a class of conjugated polymer with excellent thermal and environmental stability[2] as well as high electrical conductivity when doped.[3] Simple, unsubstituted polythiophenes are infusible materials and present processing challenges. The incorporation of lateral pendant groups in polythiophenes has become a common strategy to make these otherwise intractable materials processable.[4] The nature of the side chains influences the polymer morphology. In asymmetrically substituted polythiophenes, the degree of regioregularity is recognized to play an important role in molecular packing, crystallization, and charge transport properties. For example, the conductivity of iodine-doped poly(3-dodecylthiophene) solution-cast films increased by a factor of 60 times from 10 S cm$^{-1}$ for regiorandom (54% H−T) to 600 S cm$^{-1}$ for regioregular (91% H−T) configurations.[5]

Conjugated polymers are appropriate for applications requiring large area, flexibility, and low cost. Current technologies for polymer thin film transistors are based on solution processing.[6] Solution processable poly(3-hexylthiophene) (P3HT) has been intensively studied, and it is known that film morphology depends upon factors like solvent, deposition conditions, polymer molecular weight, degree of regioregularity, density of molecular defects, and thermal history. The solvent-cast film morphology generally comprises a mixture of lamellar crystallites and amorphous interlamellar regions. This polycrystalline morphology contains thin (∼10 nm) platelet-like crystallites limited to a few microns in lateral extent that results in a high density of crystal−amorphous boundaries. Inside the lamella, chains are $\pi$-stacked with respect to one another, chain axes lie approximately normal to the plane of the platelet, and for thin films chain axes lie parallel to the substrate.

Several studies have assessed the impact of molecular, structural, and processing parameters on charge transport in solution deposited polycrystalline thin films of regioregular P3HT. Higher hole mobility was found for samples with higher regioregularity and in-plane $\pi$-stacking of the backbones.[7] The mobility has been reported to increase with increasing degree of regioregularity and increasing molecular weight.[8] McGehee and collaborators found an enhancement in charge carrier mobility from $1.7 \times 10^{-6}$ to $9.4 \times 10^{-3}$ cm$^2$ V$^{-1}$ s$^{-1}$ for respective molecular weights of 3.2 and 36.5 kDa in thin films of regioregular P3HT.[9] In that study, higher mobilities were found for higher molecular weights in spite of the fact that the lower molecular weight samples presented a higher degree of crystallinity. This result was attributed to less defined crystalline regions and to longer chains serving as connective transport pathways between ordered domains in higher molecular weight samples.

In general, the presence of interfaces and amorphous regions between adjacent crystalline regions appears to be a major limiting factor for charge transport in thin films of conjugated polymers. Many techniques to promote chain alignment have been proposed to overcome isotropic polycrystalline morphologies that contain numerous interfaces/amorphous regions and take advantage of the intrinsic anisotropic nature of the individual conjugated polymer chains in a globally oriented sample. These approaches include the following: rigid chain-flexible chain binary blends (using ultrahigh-molecular-weight polyethylene),[10] epipolymerization of a monomer film deposited by sublimation onto an alkali halide substrate,[11] alignment of liquid-crystal rigid chain−solvent phases on mechanically rubbed[12] or photoaligned[13] polyimide substrates, unidirectional rubbing a previously spin-coated conjugated polymer film,[14] Langmuir−Blodgett techniques combining the possibility to control the thickness of the conjugated polymer film on the liquid surface with the ability to induce a preferential orientation of backbones along the dipping direction during film transfer onto a substrate,[15] block copolymer rigid-rod coassembly under a bias field to induce uniaxial alignment of the guest,[16] soft lithography combined with solventless polymerization in channels to produce oriented polyacetylene films,[17] preferential orientation of chains along the long axis of the channels via embossing conjugated polymer films within the channels of a silicon mold,[18] friction transfer to form a highly oriented single crystal-like morphology of poly(9,9-dioctylfluorene) films,[19] dissolving conjugated polymers into nematic liquids to form extended networks,[20] supramolecular assembly of conjugated polymers,[21] simultaneous orientation and conversion of a soluble precursor polymer,[22,23] and preparation of ribbon-like nanofibers (whiskers) by means of crystallization in poor solvent solutions.[24] Finally, directional eutectic solidification, a technique to direct the assembly of crystallizable polymers[25] as well as crystallizable block copolymers,[26] has recently been applied to regioregular P3HT.[27]

* To whom correspondence should be addressed. E-mail: elt@mit.edu.
[†] Department of Materials Science and Engineering.
[‡] Department of Chemistry.

10.1021/ma8020739 CCC: $40.75 
Published on Web 11/21/2008

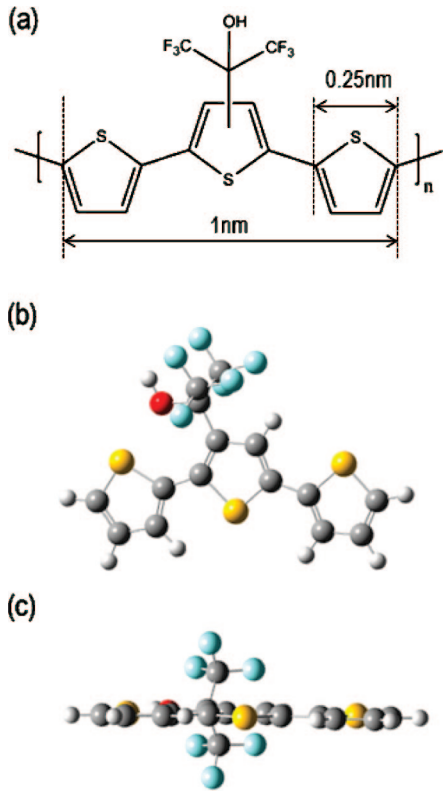


**Figure 1.** (a) Molecular structure of regiorandom HFIP-PT. The pendant group repeats every three units along the chain. The average number of repeat units per chain corresponds to 24 and 44 for the 10 and 18 kDa molecular weight samples, both with a polydispersity index of 2.4. (b) Side view and (c) bottom view of the minimized structure of HFIP-PT terthiophene monomer. The symmetry of the HFIP pendant group is probably assisting in backbone planarization.[36]

In this contribution, we report on a strategy to obtain highly oriented films of hexafluoroisopropanol functionalized polythiophene (HFIP-PT) by initial formation of a gel followed by melting and shear processing. The incorporation of HFIP, a strong and stable dipolar group, to the PT backbone enhances the solubility and especially the hydrogen bond forming capabilities of the polymer. HFIP-PT can form a self-supporting network structure through a possible combination of polymer−polymer chain interactions and interchain associations through HFIP pendant groups promoted by addition of small polar protic molecules such as methanol and water to a HFIP-PT/tetrahydrofuran (THF) solution. The reversibility of these physical cross-links allows the gel to melt and to plastically deform. Optical analysis of oriented gel films reveals highly anisotropic morphologies. Further structural analysis by means of electron and X-ray diffraction suggests an uniaxial alignment of $\pi$-stacked chains in the most densely packed regions.

## Experimental Section

**Materials.** The molecular structure of poly(3′-hexafluoroisopropanol-2,2′:5′,2′′-terthiophene) is shown in Figure 1. HFIP is a strong hydrogen bond donor group often used in chemical sensing such as for the detection of phosphate esters common to chemical warfare agents.[28] It was synthesized via oxidative polymerization from the terthiophene monomer. Thermal analysis indicates that HFIP-PT presents a melting peak at 208 °C (see Figure S1 in the Supporting Information). The analysis of the nuclear magnetic resonance (NMR) data reported earlier[29] ($^1$H (300 MHz, $CDCl_3$) $\delta$: 7.26 (aromatic C−H), 7.19 (aromatic C−H), 7.15 (aromatic C−H), 3.97 (O−H)) indicates that HFIP-PT is regiorandom. Hence, the average repeating unit of HFIP-PT presents 50% of the HFIP group in each possible position, introducing an effective mirror plane normal to the chain axis at the center of the terthiophene monomer. Two batches of HFIP-PT were used in this study, one with an $M_n$ of 10 kDa and another with an $M_n$ of 18 kDa, both with a polydispersity index of 2.4. The average number of repeat units per chain corresponds to 24 and 44 for the two molecular weight samples. The 10 kDa HFIP-PT was used in the study of the gelation mechanism, and the 18 kDa batch was mostly used to prepare thin films.

**Techniques.** NMR spectroscopy was conducted using a Varian Mercury ($^1$H, 300 MHz, $CDCl_3$). Fourier transform infrared (FTIR) spectroscopy was performed on a Perkin-Elmer 2000 using KBr window cards as support (Sigma Aldrich, real crystal IR). Differential scanning calorimetry (DSC) analysis was conducted on a Q10 V9.0 TA Instrument. Film thickness was evaluated on a Tencor P-10 surface profilometer. Light microscopy (LM) analysis was done employing a Zeiss Axioskop and a Zeiss Axioskop 2. Thermal stability and optical anisotropy of oriented thin films were evaluated with regard to variations of the intensity of reflected polarized light on a LM with an Oriel spectrophotometer attached. The maximum intensity of reflected polarized light corresponds to the chains being aligned parallel to the polarizing filter (45°) and the minimum when oriented at plus or minus 45° with respect to the filter (0° and 90°). Changes in the intensity of reflected light were correlated to the degree of in-plane optical anisotropy by rotating the film on the LM stage. Thermal treatment was conducted on a Linkam THMS600 stage with TP94 single ramp temperature controller coupled to the LM. Transmission electron microscopy (TEM) was performed on a JEOL 2000FX and on a JEOL 2011. Both instruments were operated at 200 kV. The vacuum in the TEM specimen chamber was $10^{-5}$ Pa. Bright-field images and diffraction patterns were recorded with an AMT camera system. Because of the beam sensitivity of the sample, TEM was performed under low dose conditions so as to have a sufficient lifetime to record diffraction patterns. Diffraction pattern calibration was done with an evaporated aluminum standard (Electron Microscopy Sciences) at the same acceleration voltage and objective lens setting. Oriented gel films suitable for TEM analysis were coated with a 25 nm carbon film on a Denton Vacuum DV-502A evaporator with a nominal vacuum of $10^{-4}$ Pa. Selected regions of carbon-coated films were detached from the glass support using poly(acrylic acid) backing (Alfa Aesar) and transferred to a standard 200 mesh TEM grid (Electron Microscopy Sciences, G200-Cu). X-ray diffraction (XRD) analysis of thin films ($2 \times 10$ mm$^2$ and 3 $\mu$m thick) oriented on glass substrates was performed on a Rigaku RTP500RC instrument operated in Bragg−Brentano geometry with Cu K$\alpha$ radiation ($\lambda$ = 0.154 nm).

**Methods.** Complete descriptions of the gelation process and the preparation of oriented thin films are given in the Supporting Information.

The gelation procedure consisted of replacing THF by methanol in an initial solution of HFIP-PT/THF via solvent interdiffusion followed by solvent evaporation inside a fume hood at room temperature and atmospheric pressure, resulting in the formation of an orange jelly-like substance. Under these conditions, ambient water is incorporated into the gel.

Oriented thin films were prepared on glass substrates by shearing the gel with a razor blade: one pass per film at an angle of ~30°. When the gel was sheared at room temperature, only the thinnest regions became oriented. Better chain alignment was obtained when the gel was sheared during cooldown after heating to 100 °C for a few seconds. When deformation was conducted close to 100 °C, shearing did not result in an anisotropic morphology. In order to attain the right conditions for deformation, it was key to cool down the molten gel, which suggests that a gel re-formation transition takes place during cooling and that it is beneficial for the orientation of the polymer.

## Results and Analysis

**Gelation Mechanism.** THF is a good solvent for HFIP-PT, methanol is a poor solvent, and water is a nonsolvent. After

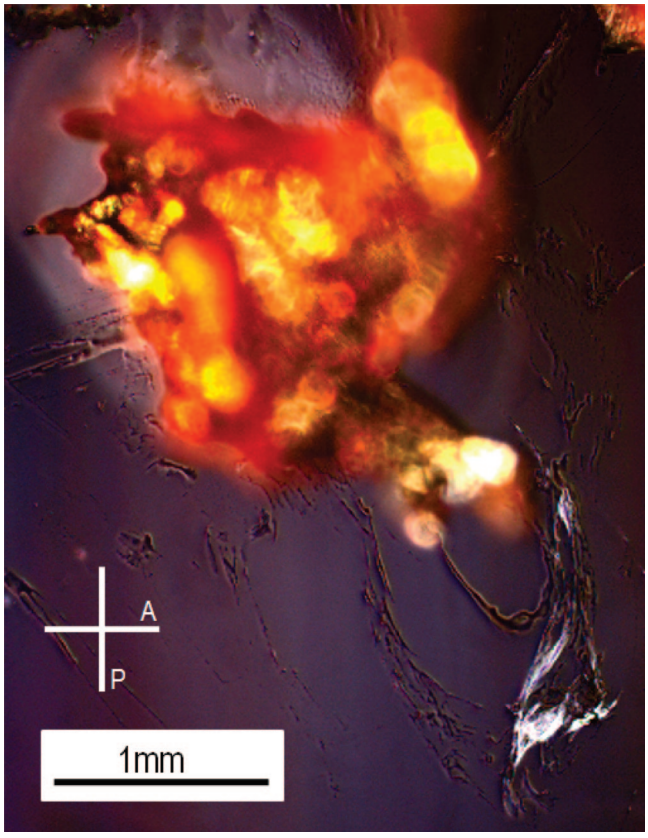


**Figure 2.** Polarized light micrograph of a piece of HFIP-PT gel deposited on a glass slide. The gel readily turns into a globally anisotropic morphology upon accidental deformation with the spatula as illustrated by the thin birefringent region at the lower-right corner.

48 h of methanol interdiffusion into the HFIP-PT/THF solution, the solution becomes turbid. The increasing concentration of methanol induces the chains to cluster, most likely due to the combined enthalpic effect of the strong $CH_3OH$−HFIP associations and polymer−polymer chain interactions. The sample is then transferred into a crucible where solvent evaporation at ambient pressure inside a fume hood results in the formation of an orange jelly-like substance (estimated polymer concentration is 2 wt %). The gel contains HFIP-PT, methanol, and water which is incorporated from the ambient moisture.

Figure 2 shows a polarized light microscopy image of the gel taken from the crucible. The depolarization of incident light suggests an isotropic distribution of locally anisotropic clusters in the bulk gel. In contrast, the strong birefringence present in the lower-right corner in Figure 2 reveals the ability of the material to easily deform into a globally anisotropic morphology (likely due to handling the gel).

In order to investigate the governing interactions behind gel formation, we use FTIR spectroscopy to follow the initial buildup in methanol concentration and then the vacuum-assisted decrease in solvent concentration. After 0.5, 1.5, 4, 24, and 48 h exposure to methanol vapors, a drop from the initial polymer THF solution is cast onto a KBr window card. FTIR analyses of the initial HFIP-PT solution in THF (0 h) and of the gel are also conducted. Further FTIR measurements are conducted to evaluate the decrease in solvent concentration upon residence under vacuum. For this, each preparation on a KBr window card is interrogated by FTIR after 2, 24, and 48 h under a vacuum of 6 Pa (0.045 Torr). Representative series of FTIR spectra as a function of decreased solvent content are reported in Figure S2 in the Supporting Information. Samples are labeled as follows: exposure time to methanol vapors/time under

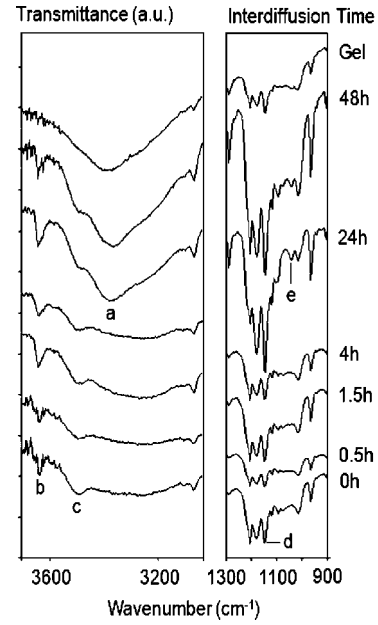


**Figure 3.** FTIR spectra as a function of solvent interdiffusion time. Spectra were taken after each sample was held for 48 h under house vacuum of 6 Pa (0.045 Torr). Specific regions of interest are labeled a−e: a: 3375 $cm^{-1}$; b: 3640 $cm^{-1}$; c: 3500 $cm^{-1}$; d: 1150 $cm^{-1}$; e: 1055 $cm^{-1}$.

vacuum; e.g., 48 h/48 h indicates the initial HFIP-PT solution in THF was exposed to methanol vapors during 48 h before being cast onto a KBr window card, which was further placed under vacuum for 48 h.

Figure 3 shows a set of FTIR spectra for the following samples: 0 h/48 h, 0.5 h/48 h, 1.5 h/48 h, 4 h/48 h, 24 h/48 h, 48 h/48 h, and gel/48 h. The left window spans a frequency range relevant to O−H stretching mode and the right window to C−O stretching mode. After 24 h interdiffusion, a broad peak emerges in the region 3600−3200 $cm^{-1}$ (labeled a) in the left window. It remains at longer interdiffusion times, and it is also evident in the gel spectrum. Its center varies between 3380 and 3366 $cm^{-1}$. The peak is located at a frequency close to the broad band found in the molten phase spectrum of *tert*-butyl alcohol (3362 $cm^{-1}$).[30] Liquid methanol exhibits a broad band centered at 3342 $cm^{-1}$. The emergence of a broad band in the 3600−3200 $cm^{-1}$ spectral region during interdiffusion of $CH_3OH$ and THF is indicative of an increased degree of hydrogen-bonding (H-bonding) network. The center of the emerging band labeled a is located at lower frequencies compared to the narrower peaks at 3640 and 3500 $cm^{-1}$ (labeled b and c, respectively). The two narrower b and c peaks could be assigned to O−H stretching in the non-H-bonding regime.[31] This interpretation seems to be further supported with the top spectrum where both the b and c peaks vanish. The absence of peaks assigned to non-H-bonded O−H stretching in the gel, jointly with the emergence of the H-bonding band, is indicative of a high degree of H-bonding between solvent molecules and HFIP groups.

In the frequency range corresponding to the C−O stretching mode, right window in Figure 3, primary alcohols appear at ∼1050 $cm^{-1}$ and tertiary alcohols are located at ∼1150 $cm^{-1}$. The peak appearing at ∼1150 $cm^{-1}$ in all spectra (labeled d) could be assigned to C−O stretching of the hydroxyl group in HFIP. Only in the spectra corresponding to longer interdiffusion times (24 and 48 h) and to the gel does a signal emerge at 1055 $cm^{-1}$, labeled e, which is assigned to the C−O stretching band of methanol. The interpretation of FTIR measurements indicates that at least one of the molecular interactions responsible for gelation is based on H-bonding associations and that methanol

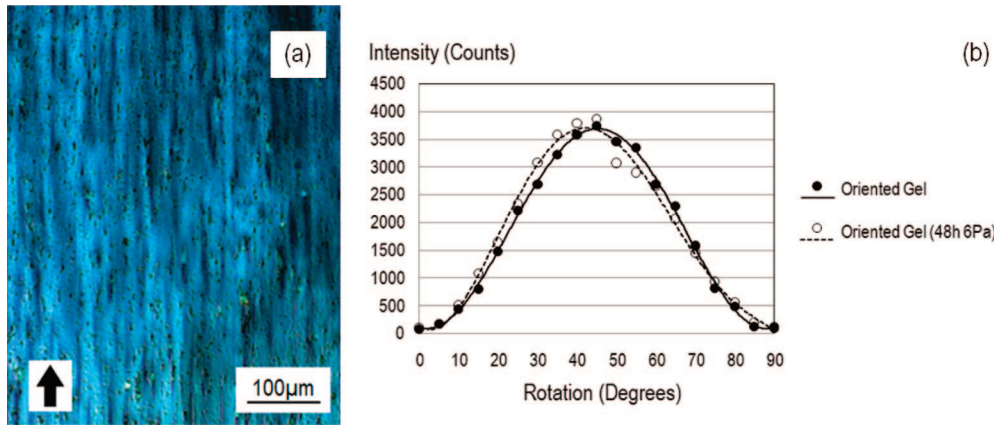


**Figure 4.** (a) Cross-polarized light micrograph of an HFIP-PT oriented gel film. The film was prepared by blade shearing the melted gel during cooldown. The shearing direction is illustrated by the arrow. The small dark entities observed are unoriented gel fragments. (b) Optical anisotropy analysis of oriented gel films. The number of counts corresponds to the intensity of the reflected polarized light at 540 nm.

is retained in the gel even after being under vacuum of 6 Pa for 48 h. HFIP-PT concentration in the gel/48 h is estimated at 88 wt %.[32]

**Oriented Gel Films.** We were motivated to find a processing pathway to form a highly oriented HFIP-PT morphology for future structure−property studies. A detailed investigation of the structure at the molecular level is sought in view of applications where a controlled orientation of the chains is relevant. Moreover, having a highly swollen but highly oriented polythiophene gel is a useful starting material for doping to create electrically conductive films and for analyte sensing films due to facile diffusion of new components into the film.

Thin films were prepared by hand shearing using a razor blade on a glass slide. The gel/0 h was first heated at 100 °C, it melted, then shearing was conducted during cooling, and an oriented gel re-formed. Oriented gel films present an essentially uniform birefringence as illustrated in Figure 4a. The changes in intensity are attributed to local variations in film thickness jointly with the presence of unoriented pieces of gel. When the melted gel is sheared immediately after heating, i.e., at a temperature close to 100 °C, the resulting film is not birefringent. This suggests that stress transfer and retention necessary to induce alignment between chains during deformation require the network of hydrogen-bonding cross-links and chain−chain interactions to build up in the system; the gel re-forms at lower temperatures.

When the gel/0 h is placed under vacuum, the solvent concentration decreases as indicated by FTIR analysis (Figure S2(c), Supporting Information). Nevertheless, the gel/48 h retains enough methanol and water to be melted and then deformed into oriented anisotropic films. This suggests an ideal gel composition consisting of a minimum content of gelling molecules at which plasticity can still be possible with minimal interference in chain packing during mechanical deformation at an optimal temperature.

The degree of in-plane optical anisotropy is quantified in Figure 4b. Analysis is conducted on two oriented films, both films prepared by shearing the molten gel (gel/0 h) during cooling from 100 °C. The film corresponding to the dashed line in Figure 4b was further placed under vacuum of 6 Pa for 48 h prior to analysis. The full width at half-maximum (fwhm) of the intensity of the reflected polarized light as a function of rotation angle for both preparations is ±23° for a sampled area of 3 mm$^2$. The simple procedure followed to prepare the films, and the presence of solvent may contribute to this misalignment.

The thermal stability of oriented films is evaluated by monitoring the variation in intensity of reflected polarized light with temperature. Sample preparation for this analysis consists on shearing the molten gel (gel/0 h) during cooldown from 100 °C and then placing the oriented film under vacuum of 6 Pa for 48 h. The results are reported in Figure S3 of the Supporting Information. Upon heating, the degree of orientation in the film drops continuously in the 55−70 °C range. No recovery of global orientation is observed upon cooling. After loss of orientation, the film can be recovered from the glass slide, reheated, and reoriented into an anisotropic morphology.

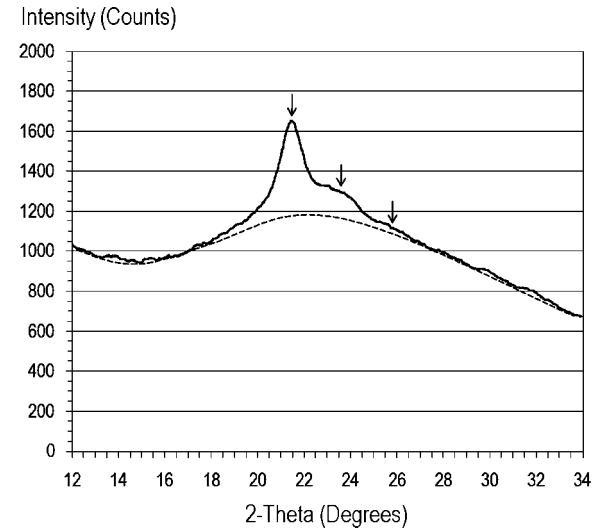


**Figure 5.** XRD analysis of an HFIP-PT oriented gel film. Three peaks are observable; the peak at lower angles would correspond to $d(h_1k_10) = 0.42$ nm spacing normal to the plane of the film and the two additional peaks at higher angles to $(h_2k_20)$ and $(h_3k_30)$, respectively.

XRD characterization of oriented gel (gel/0 h) films (2 × 10 mm$^2$ and 3 $\mu$m thick) shows a peak maximum corresponding to an interplanar spacing of 0.42 nm normal to the plane of the film and two additional peaks at higher angles, as illustrated in Figure 5. These three peaks would correspond to $(h_1k_10)$, $(h_2k_20)$, and $(h_3k_30)$, respectively. The fwhm for the $(h_1k_10)$ peak is 1° (instrumental fwhm at this angle is 0.1°). Two factors that could contribute to peak broadening are a distribution of *d*-spacings normal to the chain axis and size broadening due to crystalline clusters of sizes below about 10 nm.

TEM analysis was done on the thinnest regions at the tapering edge of a shear oriented gel (gel/0 h). These regions have likely undergone the greatest deformation. Films suitable for TEM analysis were coated with a 25 nm carbon film. Selected regions of carbon-coated films were detached from the glass support using poly(acrylic acid) backing and transferred to a standard

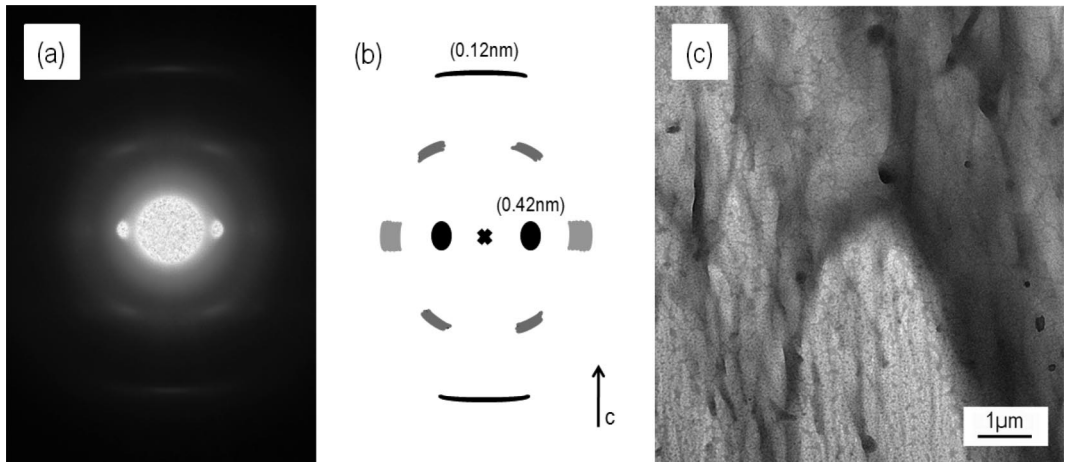


**Figure 6.** (a) Electron diffraction pattern of an oriented HFIP-PT film. Contrast has been digitally enhanced. (b) Schematic of the sheared film diffraction pattern. Labeled reflections have distances corresponding to spacings in direct space. The strong equatorial and meridional reflections are representative of a parallel stacking of uniaxially aligned chains in the plane of the film. (c) Bright-field TEM micrograph corresponding to the area contributing to the diffraction pattern. An overall aligned texture is evident with mass thickness contrast arising from thickness variations of the film.

TEM grid. The electron diffraction pattern in Figure 6a corresponds to the normal projection along the chain axis. This analysis indicates that the HFIP-PT chains lie in the plane of the film and that they are highly aligned parallel to the deformation direction. The direction along the chain axis is assigned to the crystallographic *c*-axis. The strong equatorial reflections are indicative of a parallel stacking of HFIP-PT chains in the plane of the film. The direction normal to the chain axis and in the plane of the film is assigned to $[h_1k_10]$ with $d(h_1k_10) = 0.42$ nm. An additional weak and diffuse equatorial reflection is observable. The spacing is around 0.21−0.24 nm, which could correspond to the second order of the strong inner reflection with spacing 0.42 nm.

In P3HT an interchain $\pi-\pi$ stacking distance of 0.38 nm is assigned between successive polythiophene backbones.[33] The fiber pattern in Figure 6a also presents strong equatorial reflections which could correspond to the parallel stacking distance between HFIP-PT conjugated backbones. The higher spacing of 0.42 nm found in HFIP-PT oriented gels compared to P3HT could be the consequence of a less dense chain packing due to the absence of regioregularity, to the size of the HFIP pendant group, and to the presence of solvent.

The arced meridional reflections in Figure 6a correspond to a period of 0.12 nm along the *c*-axis. This distance is approximately half the width of one thiophene ring (see Figure 1). This periodicity along the chain axis suggests that the conjugated backbones are shifted with respect to each other neighbors by half the thiophene length, yielding an interdigitation of the pendant groups. The regiorandom nature of HFIP-PT and the steric interactions between HFIP groups could contribute to the axial shift between neighboring chains. The meridional reflections give an azimuthal arcing of approximately ±10°, which corresponds to less than half the magnitude obtained from the optical anisotropy analysis in the LM. This is likely due to the increased amount of shearing in the thinnest regions of the film and the smaller sampled area (selected area for diffraction in the TEM was 100 $\mu m^2$ while in the optical anisotropy analysis in the LM was 3 $mm^2$). Additional diffuse reflections are observable with spacing around 0.20−0.23 nm. The presence of these (*hkl*) reflections suggests a three-dimensional order in oriented gel films.

The rigid nature of the HFIP-PT chains, polymer−polymer interactions, and the proximity of the hydroxyl group in HFIP to the PT backbone allow chains to align upon mechanical orientation. The lack of regioregularity, however, is a limiting factor to achieve a full crystallographic registry between stacked chains and possibly to attain an overall crystalline configuration except in the most densely packed regions. Figure 7 is a model of the morphology of oriented gel films and of the local arrangement of chains and small molecules in the highly oriented clusters. In Figure 7a only the distribution of HFIP-PT chains is depicted; we suggest the existence of tie points in the form of ordered clusters in an overall swollen network. Figure 7b summarizes the analysis of the highly oriented regions: (1) HFIP-PT chains lie in the plane of the film, (2) there is a parallel $\pi-\pi$ stacking of uniaxially aligned backbones, and (3) a network of linkages based on chain−chain interactions and H-bonding associations between HFIP groups and small polar protic molecules is necessary for stress transmission and retention upon mechanical orientation during gel re-formation from the molten state.

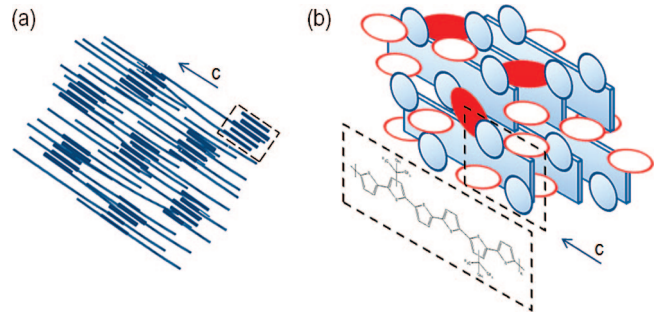


**Figure 7.** (a) Model of the morphology of HFIP-PT oriented gel films suggesting an anisotropic distribution of ordered clusters in an overall swollen network (only polymer chains are depicted; *c*-axis lies in the plane of the film). Thicker segments represent a more dense packing between chains in the crystalline clusters. While chains in between ordered regions are depicted in a rigid-like configuration, the high concentration of solvent in these regions is expected to limit their crystallinity. (b) Molecular packing in the crystalline clusters. The strips (blue) represent the PT backbones and the attached ovals (blue) the HFIP pendant groups. The elongated darker ovals (red) connecting pendant groups represent the reversible cross-links based on hydrogen-bonding associations between HFIP pendant groups mediated by polar protic molecules (methanol and water). The elongated ovals (white) represent solvent molecules interleaving between chains. The proximity between conjugated backbones is representative of the effect of direct polymer−polymer associations.

The crystalline regions in HFIP-PT gels appear similar to the crystal−solvate phases observed in certain solutions of rigid polymers. Papkov and co-workers promoted the concept of

crystal−solvate to describe the cocrystallization of rigid polymers and solvent molecules.[34] Rigid polymers can also form crystal−solvate phases with oligomeric solvents, such as the case of poly(*p*-phenylene benzobisthiazole) solutions in poly(phosphoric acid). In this system, Thomas and Cohen observed a phase transition to the solid state driven by the action of water as coagulant during film and fiber spinning from a poly(phosphoric acid) solution in the nematic state, resulting in highly oriented parallel packing of polymer and oligomer phosphoric acid chains.[35]

## Conclusion

Hexafluoroisopropanol functionalized polythiophene is able to build up a self-supporting network structure based on a combination of polymer−polymer chain interactions and the association of HFIP pendant groups with small polar protic molecules through hydrogen bondings. These thermally reversible physical cross-links incorporate plasticity into the conjugated polymer gel. Under balanced combination of mechanical stress and temperature, the gel can be processed into thin films with the chains highly aligned along the shearing direction. We suggest the gel morphology comprises a distribution of crystalline clusters in an overall swollen network. In these ordered regions conjugated backbones are $\pi$-stacked with respect to each other neighbors and lie parallel to the substrate. The mechanically induced structural rearrangement from an isotropic to an anisotropic conjugated polymer gel occurs when transitioning from the molten state to the gel state.

**Acknowledgment.** This work was supported primarily by the MRSEC Program of the National Science Foundation under Award DMR 02-13282. T.M.S. and F.W. are grateful for financial support from the National Science Foundation, ECCS-0731100. We thank Dr. Scott A. Speakman for his help in the X-ray diffraction part of this work.

**Supporting Information Available:** Experimental details. This material is available free of charge via the Internet at http://pubs.acs.org.

## References and Notes

(1) *Handbook of Conducting Polymers*; Skotheim, T. A., Reynolds, J. R., Eds.; CRC Press: Boca Raton, FL, 2007.
(2) Wang, Y.; Rubner, M. F. *Synth. Met.* **1990**, *39*, 153.
(3) See e.g.: *Handbook of Oligo- and Polythiophenes*; Fichou, D., Ed.; Wiley-VCH Verlag GmbH: Weinheim, Germany, 1999; Chapter 2.
(4) Elsenbaumer, R. L.; Jen, K. Y.; Oboodi, R. *Synth. Met.* **1986**, *15*, 169.
(5) McCullough, R. D.; Lowe, R. D. *Chem. Commun.* **1992**, 70.
(6) Forrest, S. R. *Nature (London)* **2004**, *428*, 911.
(7) Sirringhaus, H.; Brown, P. J.; Friend, R. H.; Nielsen, M. M.; Bechgaard, K.; Langeveld-Voss, B. M. W.; Spiering, A. J. H.; Janssen, R. A. J.; Meijer, E. W.; Herwig, P.; De Leeuw, D. M. *Nature (London)* **1999**, *401*, 685.
(8) Sirringhaus, H. *Adv. Mater.* **2005**, *17*, 2411.
(9) Kline, R. J.; McGehee, M. D.; Kadnikova, E. N.; Liu, J. S.; Frechet, J. M. J. *Adv. Mater.* **2003**, *15*, 1519.
(10) (a) Andreatta, A.; Smith, P. *Synth. Met.* **1993**, *55*, 1017. (b) Montali, A.; Bastiaansen, C.; Smith, P.; Weder, C. *Nature (London)* **1998**, *392*, 261.
(11) Thierry, A.; Mathieu, C.; Straupe, C.; Wittmann, J. C.; Lotz, B.; Da Costa, V.; Le Moigne, J. *Macromol. Symp.* **2001**, *166*, 43.
(12) (a) Redecker, M.; Bradley, D. D. C.; Inbasekaran, M.; Woo, E. P. *Appl. Phys. Lett.* **1999**, *74*, 1400. (b) Grell, M.; Knoll, W.; Lupo, D.; Meisel, A.; Miteva, T.; Neher, D.; Nothofer, H. G.; Scherf, U.; Yasuda, A. *Adv. Mater.* **1999**, *11*, 671.
(13) Sakamoto, K.; Usami, K.; Uehara, Y.; Ushioda, S. *Appl. Phys. Lett.* **2005**, *87*, 211910.
(14) Hamaguchi, M.; Yoshino, K. *Appl. Phys. Lett.* **1995**, *67*, 3381.
(15) Cimrova, V.; Remmers, M.; Neher, D.; Wegner, G. *Adv. Mater.* **1996**, *8*, 146.
(16) Breen, C. A.; Deng, T.; Breiner, T.; Thomas, E. L.; Swager, T. M. *J. Am. Chem. Soc.* **2003**, *125*, 9942.
(17) Gu, H.; Zheng, R.; Zhang, X.; Xu, B. *Adv. Mater.* **2004**, *16*, 1356.
(18) Hu, Z.; Muls, B.; Gence, L.; Serban, D. A.; Hofkens, J.; Melinte, S.; Nysten, B.; Demoustier-Champagne, S.; Jonas, A. M. *Nano Lett.* **2007**, *7*, 3639.
(19) Misaki, M.; Ueda, Y.; Nagamatsu, S.; Yoshida, Y.; Tanigaki, N.; Yase, K. *Macromolecules* **2004**, *37*, 6926.
(20) Hoogboom, J.; Swager, T. M. *J. Am. Chem. Soc.* **2006**, *128*, 15058.
(21) Kubo, Y.; Kitada, Y.; Wakabayashi, R.; Kishida, T.; Ayabe, M.; Kaneko, K.; Takeuchi, M.; Shinkai, S. *Angew. Chem., Int. Ed.* **2006**, *45*, 1548.
(22) Edwards, J. H.; Feast, W. J. *Polymer* **1980**, *21*, 595.
(23) Granier, T.; Thomas, E. L.; Gagnon, D. R.; Karasz, F. E.; Lenz, R. W. *J. Polym. Sci., Part B: Polym. Phys.* **1986**, *24*, 2793.
(24) (a) Samitsu, S.; Shimomura, T.; Heike, S.; Hashizume, T.; Ito, K. *Macromolecules*, **2008**,ASAP article, 10.1021/ma801128v. (b) Ihn, K. J.; Moulton, J.; Smith, P. *J. Polym. Sci., Part B: Polym. Phys.* **1993**, *31*, 735.
(25) Wittmann, J. C.; Manley, R. St. J. *J. Polym. Sci., Part B: Polym. Phys.* **1977**, *15*, 1089.
(26) De Rosa, C.; Park, C.; Thomas, E. L.; Lotz, B. *Nature (London)* **2000**, *405*, 433.
(27) Brinkmann, M.; Wittmann, J. C. *Adv. Mater.* **2006**, *18*, 860.
(28) Amara, J. P.; Swager, T. M. *Macromolecules* **2005**, *38*, 9091.
(29) Wang, F.; Gu, H.; Swager, T. M. *J. Am. Chem. Soc.* **2008**, *130*, 5392.
(30) *The Aldrich Library of FT-IR Spectra*; Pouchert, C. J., Ed.; Aldrich Chemical Company: Milwaukee, WI, 1985.
(31) *Encyclopedia of Analytical Chemistry*; Meyers C. J., Ed.; John Wiley & Sons Ltd.: New York, 2000.
(32) Estimate based upon: Nam, J.; Huang, Y.; Agarwal, S.; Lannutti, J. *J. Appl. Polym. Sci.* **2008**, *107*, 1547 After 24 h at less than 30 Torr and room temperature the amount of HFIP released in gelatin based fibers decreased from 114 to 14 ppm, a factor of 8.
(33) Prosa, T. J.; Winokur, M. J.; Moulton, J.; Smith, P.; Heeger, A. J. *Macromolecules* **1992**, *25*, 4364.
(34) Papkov, S. P. *Adv. Polym. Sci.* **1984**, *59*, 75.
(35) (a) Cohen, Y.; Thomas, E. L. *Macromolecules* **1988**, *21*, 433. (b) Cohen, Y.; Thomas, E. L. *Macromolecules* **1988**, *21*, 436.
(36) Computations were obtained using GAUSSIAN 03, Gaussian, Inc., Wallingford, CT, 2004.
(37) From ref 29: After HFIP-PT was polymerized with anhydrous iron trichloride in chloroform, the mixture was diluted with tetrahydrofuran, reduced with sodium thiosulfate, then washed sequentially with water, hydrazine aqueous solution, water, and brine, dried over $MgSO_4$, filtered with a 0.2 ìm PTFE filter, and partially evaporated under reduced pressure. The polymer solution was then precipitated into hexane. The precipitate was isolated by centrifugation and decantation of the liquid. The precipitate was dissolved in tetrahydrofuran and precipitated into hexane again. The precipitation was repeated once more. The material was dried under vacuum to yield an orange-red solid.

MA8020739